Electronic Properties of Metal-Modified DNA Base Pairs

Giorgia Brancolini and Rosa Di Felice*

National Research Center on nanoStructures and bioSystems at Surfaces (S3) of INFM-CNR, Via Campi 213/A, 41100 Modena, Italy

Received: July 21, 2008; Revised Manuscript Received: September 8, 2008

The electronic properties of several metal-modified Watson−Crick guanine−cytosine base pairs are investigated by means of first-principle density functional theory calculations. Focus is placed on a new structure recently proposed as a plausible model for building an antiparallel duplex with Zn−guanine−cytosine pairs, but we also inspect several other conformations and the incorporation of Ag and Cu ions. We analyze the effects induced by the incorporation of one metal cation per base pair by comparing the structures and the electronic properties of the metalated pairs to those of the natural guanine−cytosine pair, particularly for what concerns the modifications of energy levels and charge density distributions of the frontier orbitals. Our results reveal the establishment of covalent bonding between the metal cation and the nucleobases, identified in the presence of hybrid metal−guanine and metal−cytosine orbitals. Attachment of the cation can occur either at the N1 or the N7 site of guanine and is compatible with altering or not altering the H-bond pattern of the natural pair. Cu(II) strongly contributes to the hybridization of the orbitals around the band gap, whereas Ag(I) and Zn(II) give hybrid states farther from the band gap. Most metalated pairs have smaller band gaps than the natural guanine−cytosine pair. The band gap shrinking along with the metal−base coupling suggests interesting consequences for electron transfer through DNA double helices.

I. Introduction

DNAs and their derivatives have been widely explored in recent years for serving as novel molecular nanowires.[1−7] Among these derivatives, metal-modified DNAs (M-DNAs) are obtained by exposing double-stranded DNA (or in some cases DNA mimics) to a concentration of transition-metal ions.[8] Whereas alkali and rare-earth cations (always present in solution) undergo solely electrostatic interactions with the nucleobases,[9,10] transition-metal cations are expected to interact with the bases also by chemical bonding.[11−14,16,17] Protocols for the synthesis of metal-modified DNAs were proposed already in the 1960s,[18] unfortunately without structural characterization by X-ray or NMR. However, M-DNAs have drawn special attention much more recently, after the drastic change observed a few years ago in the conductivity of DNA when hydrogen-bonding base pairing was replaced by metal-mediated base pairing.[19] The authors suggested that one Zn(II) cation couples to each base pair by replacing the proton at the N1 site of purines (Figure 1). Since then, different kinds of M-DNAs have been synthesized and have shown promising features for potential applications in nanotechnology.[19−24] Despite the difficulties encountered so far to reproduce the first result that reported the metallic behavior of Zn-DNA[19] due to technical hurdles in the control of synthesis procedures, structural characterization, and transport measurements, there are still big expectations that metal doping of DNA can produce good molecular wires.[13,14,16,25,26] The changes induced by metal incorporation are supposed not only to affect the structure of the double strand but also to confer a variety of metal-based functionalities to DNA, resulting in special functions such as enhanced conductivity,[19] magnetic properties,[22,27] and possibly others.

Besides the recent interest by the nanotechnology community, the binding of transition-metal cations to DNA has been a subject of intense research for several years for its biochemical relevance.[10,18,28−37] Among these ions, zinc and copper are essential elements in biology. Specifically, numerous enzymes are known to employ these ions in the processes of replication, transcription, and translation. For example, zinc plays a role in conformational changes that occur within the DNA structure.[38] Furthermore, several proteins use metal cations to stabilize the DNA design. It thus emerges that gaining knowledge on the interaction of metal cations with nucleobases is of evident importance in both life and materials science. Metalated nucleotides could be used as M-DNA-based nanodevices[13,14,16,19,23,24] and various functional drugs.[39,40]

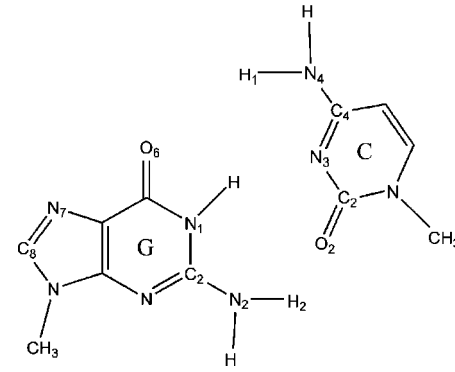

Figure 1. Naming of atomic sites in the natural GC pair.

Although the partnership between metal cations and nucleobases is of paramount importance in so diverse fields and has been studied for several years, the questions on how and to what extent the metal embellishes the DNA bases are still open. Much effort has been devoted to explaining basic issues such as the coordination properties of metal cations, the thermal stabilization, and the influence on the DNA structures.[10,32−34] Experimentally, some model compounds have been studied by means of synthesis and structural characterization.[19,20,28−31] Theoreti-

* To whom correspondence should be addressed.

10.1021/jp806419t CCC: $40.75
Published on Web 10/24/2008

cally, classical molecular mechanics and dynamics simulations, as well as quantum chemical calculations with limitations to simplified models, were employed to study the coupling of metal cations with DNA nucleobases.[11−14,16,17,37,39−41] Much work revealed a preferential coupling of cations to the N7 site (Figure 1) of guanine or adenine, which does not comply with the recent suggestion that in metallic M-DNA, Zn(II) ions alter the hydrogen-bonding patterns by substituting for protons at the N1 site of purines.[19] This structural dilemma was complicated by the absence of clear-cut X-ray structural characterization and by the shortcomings of standard theoretical methods based on density functional theory (DFT) in predicting geometries that involve nonbonding interactions. Besides, also classical molecular dynamics simulations, which are reliable for structural predictions of nucleic acids, are not helpful in the case of M-DNA because of the lack of reliable force fields for the treatment of transition-metal cations in a nonstandard situation. Only quite recently have the results of DFT calculations been able to present convincing evidence of viable geometries for Zn(II)-metalated guanine−cytosine (GC) base pairs compatible with the experimental clue about the breaking of hydrogen bonds and proposed stuctures of such pairs that can form double helices with altered hydrogen-bonding motifs.[14] In addition, only two studies[11,12] have analyzed the interaction of Cu(II), a d^9 open-shell cation, with guanine, but its influence on base pairing and electronic properties was not considered in depth. We take inspiration from the recently proposed configurations with Zn(II) ions incorporated into the axis of the double helix[14,16] and extend the study of similar geometries to other cations, namely, Ag(I), Cu(I), and Cu(II). The main goal of this paper is to unravel possible fingerprints of metal−base hybridization for some metal species, thus identifying which metal elements are most suitable to perturb the electronic structure of DNA in a profitable way for nanotechnology applications. To do this, comparison of the behaviors of different elements must be done on results obtained at the same level of theory and with the same computational scheme; hence, also Zn(II) ions are re-examined by us.

We present and discuss the results of a first-principle DFT study of several metal-mediated M^{n+}−GC complexes (M = Zn, Ag, Cu; n = 1, 2) in the gas phase. We find that all of the examined metal species are capable of binding guanine−cytosine (GC) base pairs in the ratio 1:1, and the resulting M^{n+}−GC pairs have a lower band gap than the Watson−Crick GC pair. Cu and Ag are more effective than Zn in hybridizing with G and C frontier orbitals and are therefore expected to be more likely to induce changes in the electron transfer properties of M-DNA relative to natural DNA.

II. Computational Details

Our computational approach is based on ab initio density functional theory with the B3LYP hybrid exchange−correlation (xc) functional.[42] Previous theoretical calculations have shown that the B3LYP approach is a cost-effective method for studying transition-metal ligand systems.[43] The standard 3-21G** 5d (B1) basis set was employed for Ag(I)−GC complexes because this is the only set available for Ag ions, whereas the standard 6-31G** (B2) basis set was employed for Zn(II) and Cu(I). For the Cu(II) complexes with the open-shell transition-metal cation, a variety of basis sets were tried, 6-31G** (B2), 6-311++G** (B3), and a "hybrid" basis set (B4) in which the 6-31+G(d) set is used for H, C, O, and N, while the copper ion cores are described by the Stuttgart ECP 10 MDF pseudopotential[44] and the wave functions of the copper valence electrons are expanded on the original set of pseudo-orbitals augmented with diffuse and polarization functions. By comparing the results obtained with different basis sets for the Cu(II)−GC complexes (see the Supporting Information), we conclude that the B3 basis set accurately describes the systems under investigation. Thus, for Cu(II)−GC, we report in the text only the results obtained with B3, while energy level diagrams and isosurface plots obtained with B2 and B4 are reported in the Supporting Information.

All of the calculations were carried out with the Gaussian 03 software package.[45] Open-shell calculations were performed using the unrestricted formalism.

All of the calculations started from a planar coordination geometry. For each metalated pair, the atomic coordinates of all of the atoms were relaxed in the search of the metastable structure identified as the local minimum of the total energy. Our goal is not simply to search for any metastable metalated base pairs but, in particular, to find metalated pairs that remain planar or for which planarity could be recovered through stacking interactions. This is based on the idea that planar models are more appropriate for building a duplex.

Recently, a comprehensive ab initio study[14] of several Zn(II)−GC models in the gas phase has been conducted. Among the nonplanar models, the authors found one that has the imino proton of the guanine N1 atom replaced with a Zn(II) ion and that requires less than 8 kcal/mol to flatten; they propose that this is a plausible model for building an antiparallel duplex. We have used this proposed structure as a starting point for Zn(II)− and Cu(II)−GC pairs. We also considered structures in which the cation binds to the N7 site of guanine because this was found as the preferential site for several cations in the past.[10−12,46] When suitable, we added water molecules to respect the favorable coordination arrangement of the ions. In particular, for Zn(II) bonded to N7, we have added five water molecules. However, in the case of Cu(II) bonded to N7, we found that even in starting with five water molecules, one of them migrates. A recent study[15] on the attachment of $[Cu(H_2O)_n]^{2+}$ complexes at the N7 site of guanine, with a number of water molecules varying between zero and five, reported several viable structures with 4 water molecules. Among those, we chose the lowest-energy one to build our Cu(II)−N7-4$a$$H_2O$ complex. We have sampled also an alternative orientation of the 4 water molecules (the structure of Cu(II)−N7-4$b$$H_2O$ is in the Supporting Information) but found it energetically unfavorable. Both Zn(II) and Cu(II) have a preferential coordination number higher than 2, different in the two species because of the different filling of the d shell.[47]

For Ag(I)−GC and Cu(I)−GC complexes, we simply replaced the imino proton with the monovalent cation, so that the coordination to GC occurred at the N1 position of guanine and N3 of cytosine. For Ag(I), we tested binding to the N7 site of guanine without H-bond breaking. The addition of one and two coordination water molecules was also considered in this case in order to include the linear and trigonal coordination geometries for the Ag(I) cation (see Supporting Information). The principal relaxed M^{n+}−GC structures are shown in Figure 2.

To unravel the metal-induced effects, we also calculated the natural H-bonded GC base pair (denoted as H−GC) with basis sets B1, B2, and B3, for comparison at the same level of accuracy. Our results for the natural pair are perfectly in line with those of well-known standard results.[48]

Single-point self-consistent calculations of the B3LYP-relaxed structures were done also with the PBE0 xc functional[49] to check the effects of a different functional on the fundamental gap

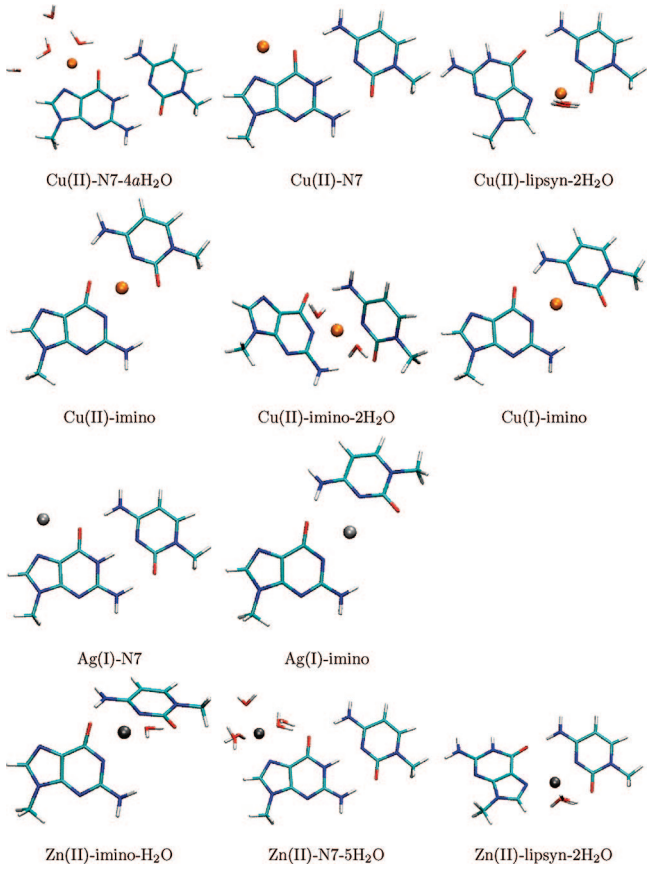

Figure 2. $M^{n+}-GC$ optimized structures at the B3LYP level, with labeling as used throughout the text.

between the highest occupied molecular orbital (HOMO) and lowest unoccupied molecular orbital (LUMO).

III. Results and Discussion

A. Structure and Stability. Selected bond lengths and angles of optimized metal-modified GC complexes are listed in Table 1. We focus our analysis on structural quantities that are representative of the degree of planarity, of the metal−base bond geometry, and of the modification of hydrogen bonds. We distinguish three different classes of metalated GC complexes. (1) Imino complexes are metalated pairs in which the imino proton of the N_1^G atom is replaced with a metal cation, with or without addition of solvation water molecules; the Watson−Crick hydrogen-bonding motif is altered. (2) N7 complexes are metalated pairs in which the Watson−Crick hydrogen-bonding pattern is maintained between guanine and cytosine and the metal cation is coordinated with the N_7^G atom in the major groove, with or without addition of solvation water molecules. (3) Lipsyn complexes are metalated pairs in which the guanine is rotated and exposes the N_7^G atom toward the cytosine, so that the metal cation bridges between the N_7 atom of guanine and the N_3 and/or O_2 atoms of cytosine.

The dihedral angle $C_4^C-N_3^C-N_1^G-C_2^G$ is representative of planarity. The analogous quantity in the pairs with the guanine in a syn conformation is the dihedral angle $C_2^C-O_2^C-N_7^G-C_8^G$. It is clear from Table 1 that the Zn-modified base pairs exhibit a stronger conformational flexibility toward out-of-plane motions as compared to that of the base pairs with the other metal species or without metal cation. This stems from the deviation of the dihedral angle from the reference value of the H−GC pair, 179.85°. In particular, we note the nonplanarity of the Zn(II)-based lipsyn complex, as opposed to that of the Cu(II)-based lipsyn complex.

TABLE 1: Selected Bond Lengths (Å) and Angles (deg) of H−GC and $M^{n+}-GC$ Structures

	H−GC	Cu(II)	Cu(II)	Cu(II)	Cu(II)	Cu(II)
label[a]		N7	N7-4aH$_2$O	lipsyn-2H$_2$O	imino	imino-2H$_2$O
symmetry[b]	P	P	NP	P	P	NP
$H_1-O_6^{G}$[c]	1.75	2.14	2.20	1.82	2.30	1.71
$H_2-O_2^{C}$[c]	1.89	1.67	1.68		3.49	2.35
N_1^G-H[c]	1.03	1.06	1.07			
N_3^C-M[c]					1.94	1.99
$M-N_1^G$[c]					1.93	1.92
N_7^C-M[c]		1.91	1.98	1.95		
$\hat{l}_1$[d]					170.3	98.8
$\hat{l}_2$[d]	177.9	177.9	176.9			
$\hat{l}_3$[d]				172.51		
$\hat{d}_1$[d]	179.9	178.6	−164.1		179.4	−120.1
$\hat{d}_2$[d]				−179.7		

	Cu(I)	Ag(I)	Ag(I)	Zn(II)	Zn(II)	Zn(II)
label[a]	imino	N7	imino	N7-5H$_2$O	imino-H$_2$O	lipsyn-2H$_2$O
symmetry[b]	P?	P	NP	NP	NP	NP
$H_1-O_6^{G}$[c]	1.68	1.82	1.67	2.04	1.81	1.77
$H_2-O_2^{C}$[c]	3.59	1.68	4.97	1.64	4.38	
N_1^G-H[c]		1.06		1.06		
N_3^C-M[c]	1.85		2.20		2.00	
$M-N_1^G$[c]	1.84		2.19		2.02	
N_7^C-M[c]		2.26		2.04		1.98
$\hat{l}_1$[d]	164.4		150.0		129.6	
$\hat{l}_2$[d]		178.8		178.8		
$\hat{l}_3$[d]						139.64
$\hat{d}_1$[d]	164.9	−179.7	143.9	−178.7	103.2	
$\hat{d}_2$[d]						−148.7

[a] The labels of the structures conform to those in Figure 1. [b] In the symmetry notation, P = planar, NP = nonplanar. [c] The superscripts G and C indicate the location of the atom on guanine and cytosine, respectively. [d] Definition of the linear and dihedral angles: $\hat{l}_1 = N_3^C-M-N_1^G$; $\hat{l}_2 = N_3^C-H-N_1^G$; $\hat{l}_3 = O_2^C-M-N_7^G$; $\hat{d}_1 = C_4^C-N_3^C-N_1^G-C_2^G$; $\hat{d}_2 = C_2^C-O_2^C-N_7^G-C_8^G$.

The quantities reported in Table 1 include the angle $N_3^C-H-N_1^G$, along with its equivalent $N_3^C-M-N_1^G$ in metalated imino pairs. This angle is an index of the linearity of the bond and significantly changes with respect to the natural pair, 177.9°, only for the nonplanar metalated complexes, Cu(II)−imino-2H$_2$O, Ag(I)−imino, Zn(II)−imino-H$_2$O. Hence, in the presently studied systems, the loss of planarity is associated with the loss of linearity of the $N_3^C-M-N_1^G$ bond. The two lipsyn geometries are a case apart, and the corresponding angles $N_3^C-M-N_7^G$ and $O_2^C-H-N_1^G$ are far from linearity in both cases.

The distances $H_1-O_6^G$ and $H_2-O_2^C$ can be inspected to monitor which metallization schemes maintain or destroy the Watson−Crick hydrogen-bonding pattern. The $H_1-O_6^G$ distance is rather well maintained; it is 1.75 Å in the natural H−GC pair and increases in the M−GC pairs by up to 30% of this value, with the largest changes occurring in the Cu(II)−GC pairs. The $H_2-O_2^C$ is instead affected by major changes upon metallization, especially for the imino pairs and the lipsyn pairs.

In the Zn(II)−imino-H$_2$O complex, the Zn(II) ion has a tetrahedral coordination, with severe distortions with respect to both planarity and linearity; in fact, the dihedral angle is 103.19°, and the $N_3^C-M-N_1^G$ angle is 129.6°. Two equivalent imino complexes can be constructed with Cu(II), either with or without water molecules, namely, Cu(II)−imino-2H$_2$O or Cu(II)−imino, respectively. In the case of these Cu(II)−GC imino complexes, the hydration shell influences the coordination of the cation with guanine. In the absence of hydration water molecules, the coordination of the Cu(II) ion is square planar with the atoms

TABLE 2: ESP Charges (Debye) of Metalated Cu(I)− and Cu(II)−GC Pairs[a]

systems[b]	Cu(II)−N7-4aH$_2$O	Cu(II)−N7	Cu(II)−lipsyn-2H$_2$O
tot charge	+2	+2	+2
Cu	0.87	1.02	0.96
$O_6^{G_c}$	−0.54 (+0.05)	−0.66 (−0.07)	−0.70 (−0.11)
$N_1^{G_c}$	−0.62 (+0.15)	−0.61 (+0.16)	−0.73 (+0.04)
$N_2^{G_c}$	−0.92 (+0.11)	−0.81 (+0.22)	−0.95 (+0.08)
$N_7^{G_c}$	−0.29 (+0.19)	−0.65 (−0.17)	−0.02 (+0.46)
$N_4^{C_c}$	−0.88 (+0.10)	−1.05 (−0.07)	−1.06 (−0.08)
$N_3^{C_c}$	−0.64 (+0.07)	−0.77 (−0.07)	−0.90 (−0.20)
$O_2^{C_c}$	−0.58 (+0.01)	−0.56 (+0.04)	−0.54 (+0.06)
$O_1^{wat_c}$	−0.70		−0.86
$O_2^{wat_c}$	−0.76		−0.86
$O_3^{wat_c}$	−0.74		
$O_4^{wat_c}$	−0.82		

systems[c]	Cu(II)−imino	Cu(II)-imino−2H$_2$O	Cu(I)−imino
tot charge	+1	+1	0
Cu	0.82	0.79	0.34
$O_6^{G_c}$	−0.54 (+0.05)	−0.61 (−0.02)	−0.53 (+0.06)
$N_1^{G_c}$	−0.74 (+0.03)	−0.76 (+0.01)	−0.60 (+0.17
$N_2^{G_c}$	−0.99 (+0.04)	−0.84 (+0.19)	−0.73 (+0.30)
$N_7^{G_c}$	−0.47 (+0.01)	−0.48 (+0.00)	−0.52 (−0.04)
$N_4^{C_c}$	−0.87 (+0.11)	−0.81 (+0.17)	−0.86 (+0.12)
$N_3^{C_c}$	−0.63 (+0.07)	−0.58 (+0.12)	−0.59 (+0.11)
$O_2^{C_c}$	−0.55 (+0.05)	−0.55 (+0.05)	−0.51 (+0.09)
$O_1^{wat_c}$		−0.69	
$O_2^{wat_c}$		−0.74	

[a] The values in parentheses are the charge variations with respect to the nonmetalated GC pair. [b] The labels of the structures conform to those in Figure 1. [c] The superscripts G and C indicate the location of the atom on guanine and cytosine, respectively.

N_1^G, O_6^G, N_3^C, and O_2^C; the N_3^C−M and M−N_1^G bond lengths are typical Cu(II)−ligand distances, and the H$_2$-O_2^C bond is practically destroyed since the final value of 3.49 Å is well beyond typical hydrogen-bonding lengths. In the presence of water, the coordination of the Cu(II) ion becomes irregular tetrahedral. The accomplishment of this geometry is accompanied by out-of-plane motions of the DNA bases that are reflected in the dihedral angle of −120.11°, the nonlinear N_3^C−M−N_1^G angle of 98.8°, and a pronounced increase of the H$_2$−O_2^C distance.

Both Cu(I) and Ag(I) have a two-fold coordination in the M−GC complexes considered by us. The Cu(I)−imino pair has minor deviations from the natural H−GC geometry, with a dihedral angle of 164.9° and a N_3^C−M−N_1^G angle of 164.4°. The Ag(I)−imino pair has instead major distortions, with a dihedral angle of 143.9° and a N_3^C−M−N_1^G angle of 150.0°.

Cu(II) can participate in N7 complexes with two different coordination schemes. In the gas phase, namely, in the absence of hydration water molecules, the coordination of Cu(II) is bidentate with the N_7 and O_6 atoms of guanine, with a strong interaction of Cu(II) with both N_7^G and O_6^G. In the four-fold Cu(II)−N7-4aH$_2$O structure, the coordination of the cation is still bidentate with both the N_7^G and O_6^G atoms,[15] whereas also a monodentate coordination with N_7 is viable (the structure of Cu(II)−N7-4bH$_2$O is in the Supporting Information). The bidentate mode was already observed for Cu(II) in a previous theoretical work.[12] N7 complexes with Zn(II) are compatible only with a monodentate conformation in which the Zn(II) ion couples to N_7^G; the six-fold coordination is then completed with the water molecules. The coordination of Ag(I) in the Ag(I)−N7 pair is similar to that of Cu(II) in the Cu(II)−N7 pair, and also the distances and angles reported in Table 1 are similar.

The lipsyn structures examined by us were derived from the recent suggestion by Fuentes-Cabrera and co-workers[14] for the Zn(II) cation, structure "Lippert syn" in their paper; on the basis of the syn mutual orientation and on the maintainance of the imino proton, the authors suggested that the "Lippert syn" model is consistent with the formation of an antiparallel duplex by stacking such pairs on top of each other. They found a nonplanar geometry for the "Lippert syn" Zn(II)−GC pair, with a rather small energy cost for flattening. We considered their same structure with a Zn(II) ion coordinated with N_7^G, N_3^C, and two H$_2$O molecules, labeled as Zn(II)−lipsyn-2H$_2$O here. We constructed the equivalent Cu(II)−lipsyn-2H$_2$O pair by simply replacing the Zn(II) ion with a Cu(II) ion. Our results for the Zn(II)−lipsyn-2H$_2$O pair are consistent with the previous ones for what concerns the deviation from planarity (see Table 1). Interestingly, for the Cu(II)−GC pair, we find instead a planar equilibrium structure. The fact that the Cu(II)−lipsyn-2H$_2$O pair is spontaneously flat suggests that it is even more suitable than the Zn(II)−lipsyn-2H$_2$O pair to form an antiparallel duplex because stacking is facilitated by planarity, and in the case of Cu(II), one saves the energy cost for flattening the base pairs.

To summarize the structural information, we find that, at odds with the highly non planar Zn(II)-GC pairs, the Ag(I)-GC and Cu(I,II)-GC pairs are almost planar structures, except for the already mentioned Cu(II)-imino-2H$_2$O complex. Assuming that only planar models are suitable for building a duplex, it is rather difficult to form antiparallel M−DNA duplexes by stacking Zn(II)−GC pairs, whereas it is much easier by stacking Cu(I,II)−GC pairs and Ag(I)−GC pairs. For realizing Zn(II)−DNA, one can assemble Zn(II)−N7-5H$_2$O pairs or Zn(II)−lipsyn-2H$_2$O pairs, paying the flattening cost in the latter case. An antiparallel Cu(II)−DNA can be built both with Cu(II)−GC pairs, where the imino proton is kept as that in Cu(II)−lipsyn-2H$_2$O, Cu(II)−N7, and Cu(II)−N7-4aH$_2$O, and with Cu(II)−GC pairs, where the imino proton is replaced by the metal cation, as in Cu(II)−imino. The same is true for Ag(I)−DNA but only when the imino proton is kept as that in Ag(I)−N7. Replacement of a hydrogen bond with a metal moiety pulls the two bases apart. Depending on the cation size, the distance between two bases is smaller in Cu−GC complexes than that in Ag−GC complexes. The metal−ligand distances for Cu(II) are larger than those for Cu(I). Note that experimentally, so far, nothing is yet available for these metal-modified structures. The possible structures described here may stimulate more synthesis and characterization efforts on these compounds.

Let us remark, finally, that we discussed above the easiness of forming M−DNA duplexes with various metals by starting from metalated pairs. Alternatively, one may want to know which pair conformations are achieved when a natural duplex is exposed to a concentration of metal cations. In this case, the results above surely suggest that the N7 complexes are attainable with all of the examined metals and oxidation states. Imino complexes are viable with Cu(II) ions but are less likely with the other cations.

Although a strict energetic comparison among all of the computed structures cannot be made because of the different numbers of atoms of the various species present in the different structures, an analysis of the formation energy of each structure with respect to the constituent isolated parts confirms the considerations above about the viability of the metalated complexes. Among the imino structures, Cu(II)−imino has the highest energy gain relative to its isolated components. The lipsyn structures Zn(II)−lipsyn-2H$_2$O and Cu(II)−lipsyn-2H$_2$O have very similar formation energies. Among the N7 structures,

TABLE 3: ESP Charges (Debye) of Metalated Ag(I)− and Zn(II)−GC Pairs[a]

systems[b]	Ag(I)−N7	Ag(I)−imino
tot charge	+1	0
Ag	0.72	0.41
O_6^{Gc}	−0.60 (−0.03)	−0.55 (+0.02)
N_1^{Gc}	−0.69 (+0.17)	−0.74 (+0.12)
N_2^{Gc}	−0.88 (+0.06)	−0.90 (+0.04)
N_7^{Gc}	−0.54 (−0.07)	−0.49 (−0.02)
N_4^{Cc}	−0.98 (−0.07)	−0.84 (+0.07)
N_3^{Cc}	−0.78 (+0.00)	−0.69 (+0.09)
O_2^{Cc}	−0.59 (+0.00)	−0.56 (+0.03)

systems[b]	Zn(II)− lipsyn-2H_2O	Zn(II)− N7-5H_2O	Zn(II)− imino-H_2O
tot charge	+2	+2	+1
Zn	0.79	0.82	0.95
O_6^{Gc}	−0.54 (+0.05)	−0.55 (+0.04)	−0.59 (+0.00)
N_1^{Gc}	−0.70 (+0.07)	−0.64 (+0.13)	−0.84 (−0.07)
N_2^{Gc}	−0.96 (+0.07)	−0.97 (+0.06)	−0.84 (+0.19)
N_7^{Gc}	−0.15 (+0.33)	−0.34 (+0.14)	−0.48 (+0.00)
N_4^{Cc}	−0.89 (+0.09)	−0.99 (−0.01)	−0.89 (+0.09)
N_3^{Cc}	−0.69 (+0.01)	−0.70 (+0.00)	−0.71 (−0.01)
O_2^{Cc}	−0.55 (+0.05)	−0.60 (+0.00)	−0.58 (+0.02)
O_1^{wat}	−0.80	−0.70	−0.75
O_2^{wat}	−0.77	−0.73	
O_3^{wat}		−0.71	
O_4^{wat}		−0.72	
O_5^{wat}		−0.69	

[a] The values in parentheses are the charge variations with respect to the nonmetalated GC pair. [b] The labels of the structures conform to those in Figure 1. [c] The superscripts G and C indicate the location of the atom on guanine and cytosine, respectively.

Cu(II)−N7 has the markedly highest energy gain. More details are given in the Supporting Information.

B. Electronic Structure: Charge Shifts, Electron Energy Levels, and Wave Functions. The inspection of the electronic structure of the metalated pairs and the comparison to that of the natural H−GC pair give us more insight into the effects induced by the complexation of the GC pair with metal cations, complementing what we have learned above from the analysis of the geometries.

Atomic charges represent useful qualitative information on the electronic structure and, in particular, on relative charges when atoms change their ligand coordination. We computed atomic charges using the ElectroStatic Potential (ESP) scheme.[50] Individual atomic charges in metalated pairs and their deviations relative to the metal-free pair are reported in Tables 2 and 3. In the Cu(II)−N7 pair, with the metal in the N_7^G position and without any hydration molecules, N_7^G becomes more negative than that in the metal-free pair; a decrease of negative charge is detected at the N_1^G and N_2^G atoms. In contrast, the screening of water molecules in Cu−N7-4*a*H_2O induces a loss of electrons at the N_7^G, N_1^G, and N_2^G atoms, with all of the net atomic charges becoming less negative. Briefly, in both cases above, the N_1^G and N_2^G hydrogen bonds shift some charge toward cytosine, whereas the N_7^G electronic environment strongly polarizes the charge of this atom in different ways in the two structures. In the Cu(II)−lipsyn-2H_2O structure, the metal induces a very important decrease of negative charge at the N_7^G atom and an increase at the N_3^C and O_6^G atoms. In the Cu(II)−GC imino complexes, both with and without water molecules, the N_4^C atom becomes less negative, and all the other atoms are not subjected to large variations, with the exception of N_2^G, which becomes significantly more positive in the presence of water molecules. In the Cu(I)−imino pair, the most significant changes occur at the N_1^G and N_2^G atoms, which both become less negative; N_3^C and N_4^C also become less negative but by a smaller amount, whereas the other charge shifts are negligible. In both the Ag(I)−N7 and Ag(I)−imino pairs, the most relevant charge shift is a loss of electrons at the N_1^G atom. A comparable electron loss occurs at the N_3^C atom only when the Ag(I) ion is at the imino position; all other charge shifts are minor. The incorporation of a Zn(II) ion induces a conspicuous electron loss at the N_7^G and N_1^G atoms in the Zn(II)−N7-5H_2O pair and an electron loss of a similar entity only at the N_2^G atom in the Zn(II)−imino-H_2O pair. The Zn(II)−lipsyn-2H_2O exibits an important decrease of negative charge only at the N_7^G atom. As expected, variations are more important for the divalent systems. As we know, guanine is the most easily oxidative base among the four bases in B−DNA. When a redox process occurs, the charges on the atoms are redistributed. Therefore, the charge deviations on guanine are likely more relevant than those on cytosine for what concerns the consequences on electron-transfer activities.

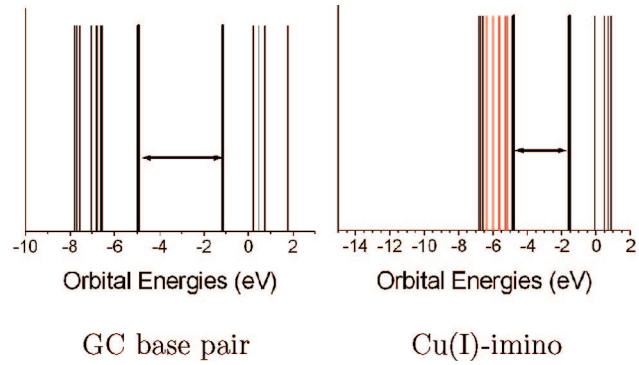

Figure 3. Orbital energy levels of the natural GC base pair and those of the Cu(I)−GC complex from B3LYP calculations with the B1 basis set. HOMO and LUMO levels are identified with thicker lines and marked by horizontal double arrows. Energy levels whose orbitals contain a metal contribution are identified in red.

A different look at the role of the metal moiety in the electronic structure of metalated base pairs can be given by inspecting the electron energy levels and the HOMO−LUMO gaps. Energy level diagrams are shown in Figures 3−5, and the HOMO−LUMO gaps are reported in Table 4. The reference H−GC structure is always included to reveal the effects of metal incorporation. The HOMO−LUMO gaps were computed with two different xc functionals, B3LYP[42] and PBE0;[49] the two functionals give different absolute values of the gaps, but the trends are consistent, and we focus in the text only on the B3LYP results. Whereas we are aware of the well-known absolute underestimation of DFT in the value of the fundamental gap,[51] we are confident that trends revealed in changes due to the incorporation of metal cations of different species and in different locations are reliable with our method. The energy gap between the HOMO and LUMO in H−GC is 3.79 eV at the DFT-B3LYP level and B2 basis set. The fundamental gap in M−GC pairs varies in different ways, shrinking in most cases and widening in a few cases. In all of the computed open-shell Cu(II)−GC pairs, the HOMO−LUMO gap decreases by different amounts depending on the conformation. The largest (and most interesting) decrease is found for the Cu(II)−N7 pair in which the gap is 0.65 eV (with the B3 basis set). The gap also decreases for the closed-shell Cu(I)−imino complex to the value of 3.23 eV. It lowers to 3.36 and 3.39 eV for Ag(I)−imino and Ag(I)−N7 complexes, respectively. In Zn(II)−GC pairs, it decreases in the case of the imino complex, in which the metal is bonded to the N_1 atom of guanine and increases in the other

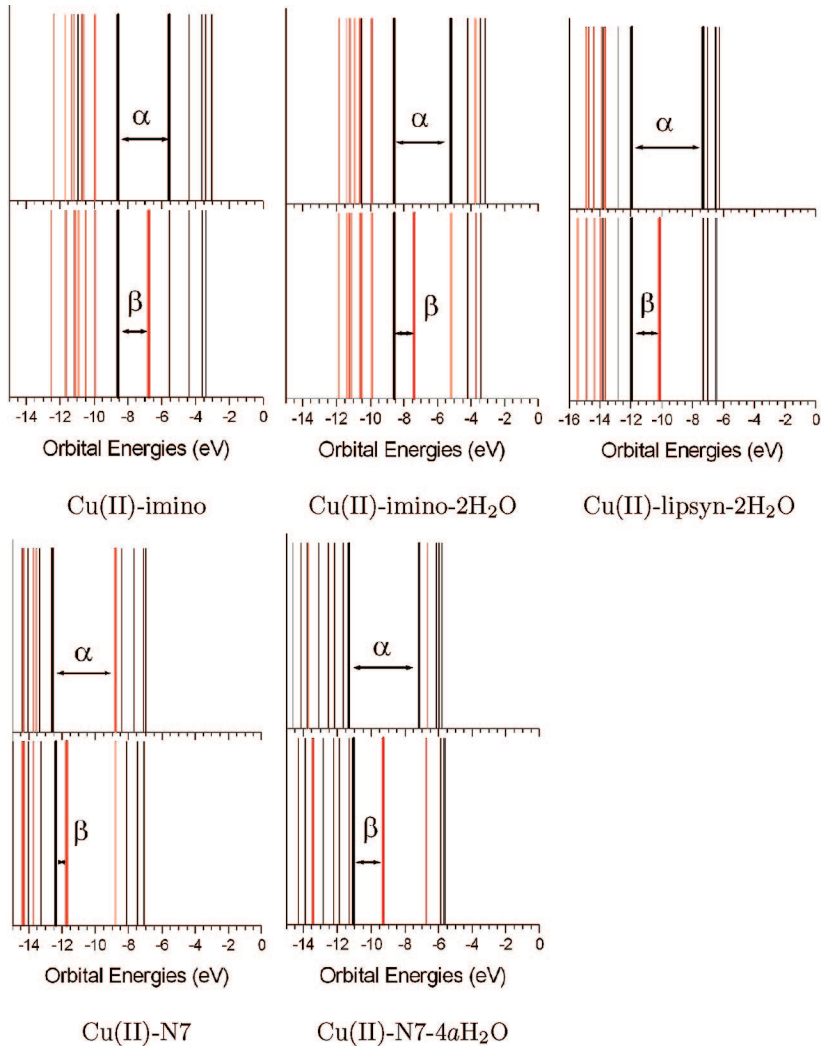

Figure 4. Orbital energy levels of the Cu(II)−N7 and Cu(II)−N7-4$a$$H_2O$ complexes from B3LYP calculations with the B3 basis set. HOMO and LUMO levels are identified with thicker lines and marked by horizontal double arrows. Energy levels whose orbitals contain a metal contribution are identified in red. Majority-spin (α) and minority-spin (β) levels are plotted separately for open-shell structures.

two cases of the lipsyn and N7 complexes, in both of which the metal cation is bonded to the N_7 atom of guanine. The energy gap change is an important metal-induced effect in view of nanotechnology applications.

As a whole, Table 4 indicates that HOMO−LUMO gap changes are much larger for the Cu(II) open-shell systems than those for the closed-shell systems. For the closed-shell systems, the identification of the HOMO−LUMO gap precisely gives an indication of the minimum excitation energy of the system. Instead, for open-shell systems, this is not straightforward, and a combined inspection of the orbitals is needed to understand which can be the lowest-energy excitation. For this purpose, in Figures 3−5, we plot the energy levels that include a metal contribution in the wave function in red color, separated in spin for the open-shell systems, and in Figures 6−10, we illustrate isosurface plots of relevant orbitals.

It is well-known,[48] and visualized in Figure 6, that in the H−GC pair, the HOMO and LUMO are localized on guanine and cytosine, respectively. The HOMO is the most chemically active state and is located on the guanine. Therefore, the interaction between a metal cation and the guanine base will definitely affect the frontier orbitals of the M−GC pairs. The chemical activity of the M−GC pairs will be somehow dependent on the metal−guanine interaction.

a. Closed-Shell Systems. Let us examine first the closed-shell systems. A glance at Figures 3−5 easily reveals that in practically all of them, the characters of the HOMO and LUMO are not affected by the presence of the metal cation. Hence, the band gap shifts are essentially due to electrostatic effects rather than orbital hybridization. Figure 10 shows that indeed for the Cu(I)−imino and Ag(I)−imino pairs, the HOMO remains on guanine and the LUMO remains on cytosine, with only a tiny component on the cation that is practically irrelevant. The HOMO−1 has a metal component in both cases. The only exception to this general behavior of closed-shell complexes is given by the Ag(I)−N7 pair, which instead has a strong metal component in the LUMO (Figure 10); anyway, the gap shrinking is comparable to that of the Ag(I)−imino pair. For the Zn(II)−GC pairs, although we do not show the orbitals, it is clear from Figure 5 that the HOMO and LUMO do not possess any metal character. Nay, no metal contribution can be detected in the occupied energy levels immediately below the HOMO. This is an indication of the fact that Zn(II) is less effective than Ag and Cu in giving electronic changes that may influence electron-transfer efficiency.

b. Open-Shell Systems. We mentioned above that the largest decreases in the value of the HOMO−LUMO gap are found for open-shell Cu(II)−GC pairs (Table 4). Let us now have a

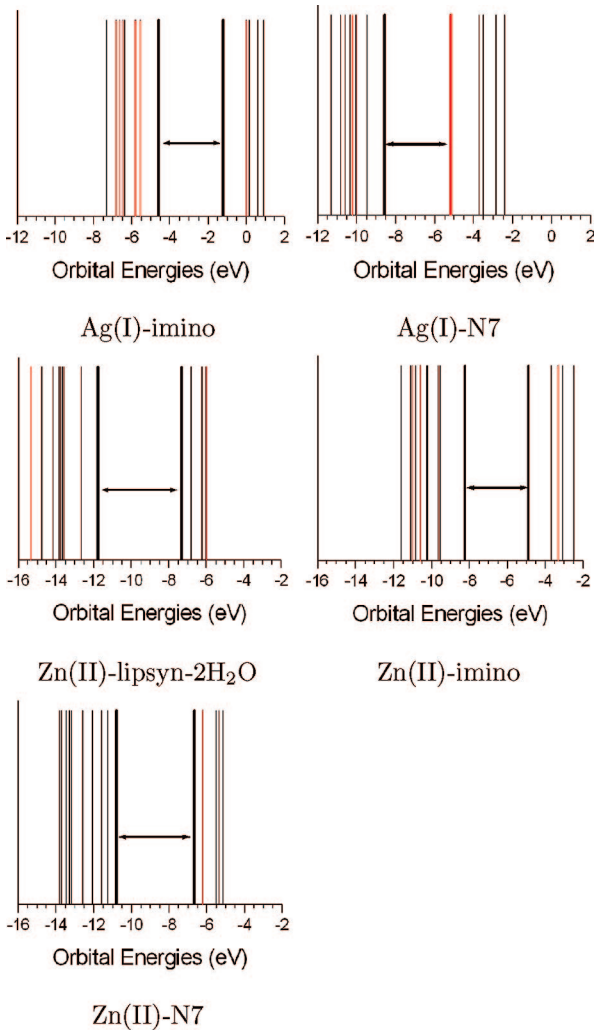

Figure 5. Orbital energy levels of Ag(I)− and Zn(II)−GC complexes from B3LYP calculations with B1 and B2 basis sets, respectively. HOMO and LUMO levels are identified with thicker lines and marked by horizontal double arrows. Energy levels whose orbitals contain a metal contribution are identified in red.

closer look at the possible allowed excitations. All of the Cu(II)−GC pairs have a β-LUMO with a metal component, Figure 4. However, neither the α-HOMO nor the β-HOMO show any metal character and are degenerate, meaning that the HOMO is doubly occupied, except in the Cu(II)−N7 system, which we discuss last. Figure 9 shows that the α-HOMO maintains its guanine character, and we verified that the β-HOMO (not shown) is identical. Therefore, the singly occupied molecular orbital (SOMO) that has the same (or similar) character as the β-LUMO and hosts the unpaired electron must be found among the majority-spin orbitals at lower energies than the fully occupied HOMO. Figure 9 shows that in the Cu(II)−imino pair, the HOMO−1 already contains a component on the cation, which however does not closely resemble the LUMO shape on Cu. In addition, the α-HOMO−1 has a degenerate β-orbital, as can be seen in Figure 4. The α-HOMO−4 instead resembles much more the Cu component of the β-LUMO and does not have a corresponding occupied β-orbital at the same energy; therefore, the α-HOMO−4 is the SOMO of the Cu(II)−imino complex. The SOMO is likely to be the most reactive orbital of the system, namely, the one that changes most if a closed-shell system is re-established by chemical reactions or voltage application. The SOMO should become either fully occupied if an electron is added to the pair

TABLE 4: HOMO−LUMO Gap Energies (eV) of H−GC and M^{n+}−GC Pairs with Two Different xc Functionals[a]

		B3LYP	PBE0
	H−GC	3.78[b], 3.79[c], 3.75[d]	4.19[b]
	Cu(II)−N7-4$a$$H_2O$	1.01 [3.32]	1.69
	Cu(II)−N7	0.65	0.83
B3	Cu(II)−lipsyn-2H_2O	1.76 [3.73]	2.46
	Cu(II)−imino	1.77 [3.87]	2.37
	Cu(II)−imino-2H_2O	1.21 [3.23]	1.81
	Cu(I)−imino	3.23	3.62
	Zn(II)−imino-H_2O	3.36	3.75
B2	Zn(II)−N7-5H_2O	4.17	4.59
	Zn(II)−lipsyn-2H_2O	4.47	4.86
B1	Ag(I)−N7	3.39	4.05
	Ag(I)−imino	3.36	3.76

[a] For H−, Ag(I)−, Cu(I)−, and Zn(II)−GC pairs, there is spin degeneracy. For the open-shell Cu(II)−GC pairs, the augmented 6-311++G** basis set is used and the HOMO−LUMO gap is found between minority-spin orbitals. The values in square brackets are for the gap between the majority-spin SOMO and the minority-spin LUMO. [b] This value was obtained for the natural H−GC pair with the B1 basis set and should be used for comparison with the results on Ag(I) complexes. [c] This value was obtained for the natural H−GC pair with the B2 basis set and should be used for comparison with the results on Cu(I) and Zn(II) complexes. [d] This value was obtained for the natural H−GC pair with the B3 basis set and should be used for comparison with the results on Cu(II) complexes.

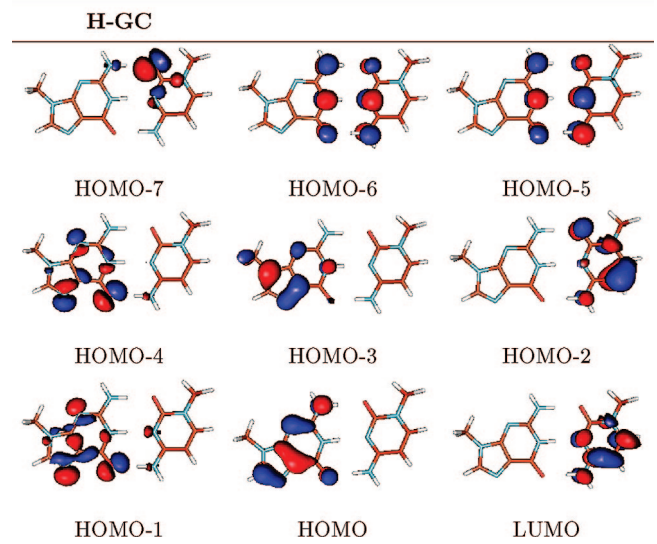

Figure 6. Isodensity contour plots of relevant orbitals around the HOMO−LUMO gap of the H−GC pair (B3LYP, B2 basis set). The situation is identical with the B1, B2, and B3 basis sets.

to occupy the β-LUMO or empty if a hole is created; in both situations, a condition of spin-degenerate doubly occupied orbitals is recovered. Within this reasoning, it becomes clear that the most significant value for the excitation gap in the open-shell systems is the energy difference between the β-LUMO and the SOMO. For all of the open-shell systems, it was evaluated as explained for the Cu(II)−imino pair. For instance, in the Cu(II)−lipsyn-2H_2O pair, the first occupied α orbital with a metal component similar to the β-LUMO and without a degenerate β counterpart is the α-HOMO−5 (Figure 9), which is the SOMO that determines the excitation gap. The SOMO−LUMO gaps are reported in square brackets at the B3LYP level in Table 4 for the open-shell complexes. The shrink of the excitation gap is definitely less pronounced than that if one looks barely at the β-HOMO−LUMO gap. However, note that the SOMO

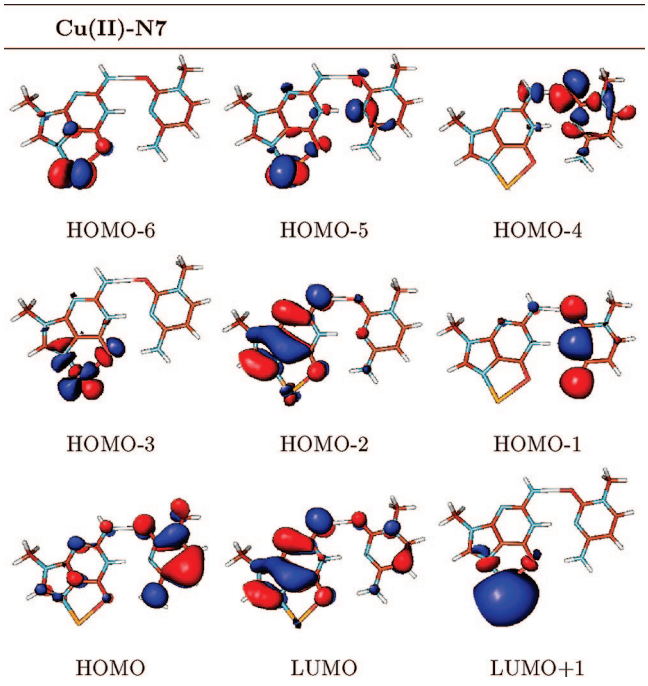

Figure 7. Isodensity contour plots of relevant majority-spin (α) orbitals and the LUMO minority-spin (β) orbital around the HOMO−LUMO gap of the Cu(II)−N7 pair (B3LYP, B3 basis set). The Cu d component is differently hybridized with guanine and cytosine in the HOMO−6, HOMO−5, HOMO−3, HOMO−2, and LUMO+1.

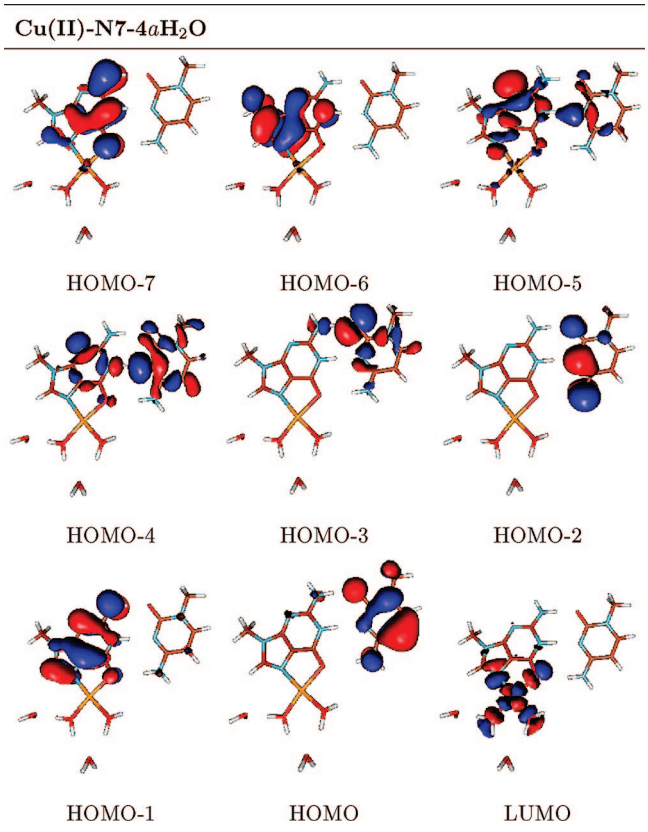

Figure 8. Isodensity contour plots of relevant majority-spin (α) orbitals and the LUMO minority-spin (β) orbital around the HOMO−LUMO gap of the Cu(II)−N7-4aH$_2$O pair (B3LYP, B3 basis set). The Cu d component is differently hybridized with guanine and cytosine in the HOMO−7, HOMO−6, HOMO−5, and LUMO.

is likely to undergo and upward energy shift upon changing to full occupation, as was discussed for other Cu redox systems.[52]

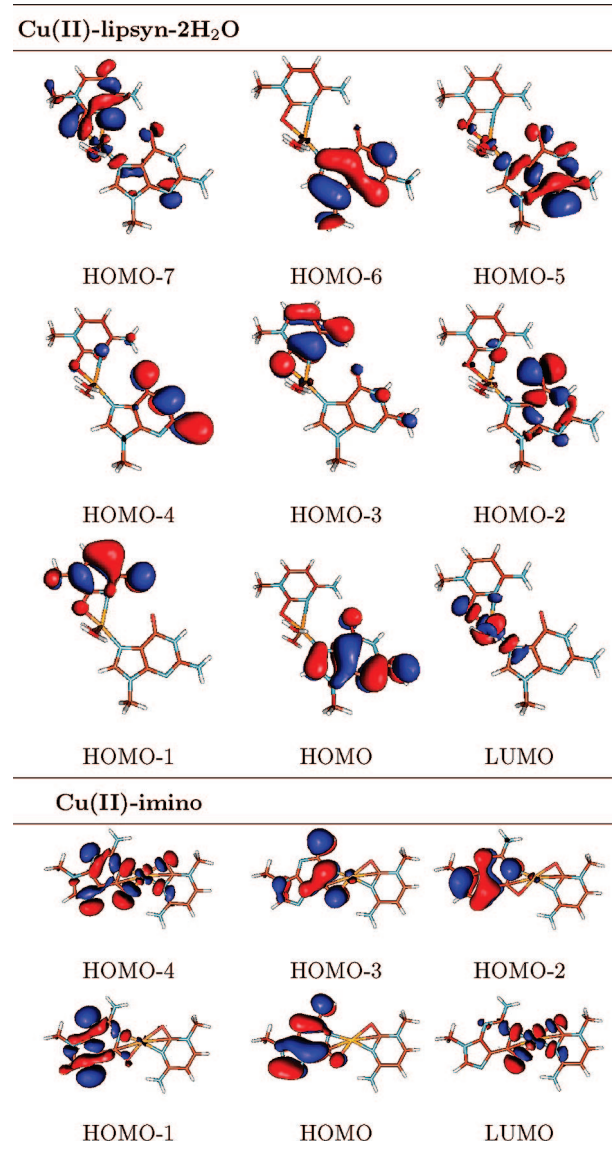

Figure 9. Isodensity contour plots of relevant majority-spin (α) orbitals around the HOMO−LUMO gap of the Cu(II)−lipsyn-2H$_2$O and Cu(II)−imino pairs (B3LYP, B3 basis set). The plotted LUMOs are minority-spin (β) orbitals and are the LUMOs of the systems. Their corresponding majority-spin components are HOMO−5 (and orbitals below) for Cu(II)−lipsyn-2H$_2$O and HOMO−4 for Cu(II)−imino, as identified from the Cu component.

The detailed account for this effect is beyond our scope here and complicated by technical hurdles in the description of a many-body problem by DFT, but we point out that it surely influences the exact value of the excitation gap that one should expect, for example, in conductance measurements.

Finally, for the most interesting cases, Cu(II)−N7 and Cu(II)−N7-4aH$_2$O where the HOMO−LUMO gaps are the smallest among all of the systems, the α-HOMO and the β-HOMO are not completely degenerate, the β-HOMO being the highest occupied orbital energy level. The HOMO−LUMO gaps in Table 4 are thus taken between the minority-spin orbitals as in all other cases characterized by α−β HOMO degeneracy. From Figure 7, in the Cu(II)−N7 system, the α-HOMO−2 is the SOMO of the system, and therefore, the α-HOMO−2-LUMO gap coincides with the SOMO−LUMO gap. This is also a system with a high energy gain and is easy to form when adding cations to an already formed duplex. We therefore predict

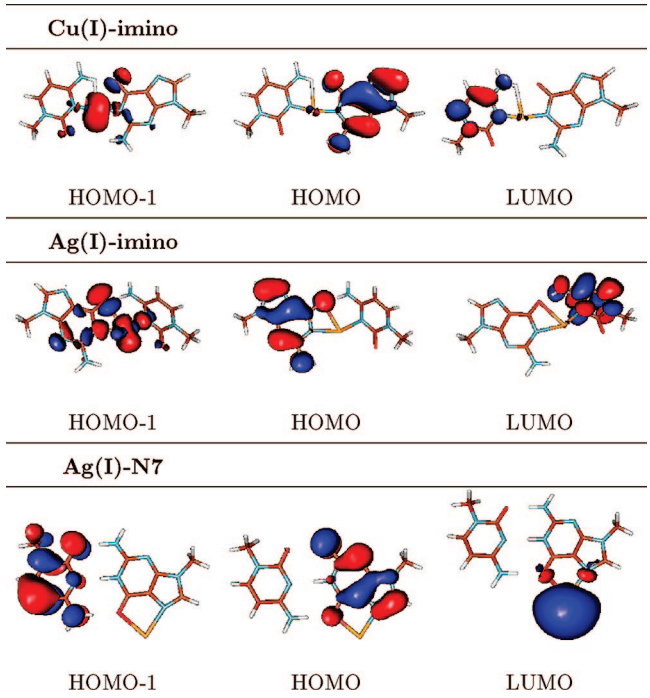

Figure 10. Isodensity contour plots of relevant orbitals around the HOMO−LUMO gap of the Cu(I)−imino (B3LYP, B2 basis set) and Ag(I)−imino (B3LYP, B1 basis set) pairs.

that the Cu(II)−N7 conformation may have enormous impact in practical applications.

We remark that in actual M−DNA-like nanostructures, the role of interplane interactions may partially affect the shape of the electron orbitals and somehow change the details of their shape. The natural aquaeous environment is also relevant and is the target of additional investigations. Notwithstanding these possible corrections, our results are sound in terms of trends of the different metals and nature of the metal−base hybridization.

IV. Conclusions

In conclusion, we have investigated the structure and the electronic properties of metal-modified GC base pairs with an ab initio DFT method by analyzing geometrical details, energy levels, and charge density distributions of the frontier orbitals. We have explored modifications with Zn(II), Ag(I), Cu(I), and Cu(II) ions, the latter of which give open-shell systems. The Zn(II)-modified base pairs exhibit large conformational flexibility toward out-of-plane motions compared to the base pair without metal cations, indicating a nonoptimal performance of such bases to form DNA helices. Cu(II) is more prone to planarity. Cu(II) is also the cation species that mostly contributes to the hybridization of the frontier orbitals. This hybridization, along with the persistent planarity, indicates that doping with Cu(II) is both structurally/energetically feasible and a powerful tool to design electronic modifications that may be exploited in applications. Cu-modified GC complexes might be the best candidates for nanowires with good conduction properties and also for on-purpose modifications of DNA to detect local electrical signals along the helix. We note also a general reduction of the HOMO−LUMO gap in complexes with Cu(I) and Ag(I).

Acknowledgment. This work was funded by the EC through projects "DNA-based Nanowires" (Contract IST-2001-38951) and "DNA-based Nanodevices" (Contract FP6-029192). Computational time on the supercomputers at CINECA (Bologna, Italy) and at NERSC (Berkeley, USA) was granted by INFM-CNR and by CNMS-ORNL, respectively. We are especially grateful to Anna Garbesi for continuous advice and discussions throughout the work, and to HouYu Zhang for participating in the early stages. We also acknowledge fruitful discussions with Felix Zamora.

Supporting Information Available: Figure SF1 and Table ST1: additional M^{n+}−GC-optimized structures and their HOMO−LUMO gaps. Table ST2: formation energies of investigated M^{n+}−GC pairs with respect to individual components. Figures SF2−SF4: energy level diagrams and isosurface plots of Cu(II)−N7 complexes obtained with different basis sets. This material is available free of charge via the Internet at http://pubs.acs.org.

References and Notes

(1) Porath, D.; Cuniberti, G.; Di Felice, R. *Top. Curr. Chem.* **2004**, *237*, 183.
(2) Di Ventra, M.; Zwolak, M. In *Encyclopedia of Nanoscience and Nanotechnology*; Singh-Nalwa, H. Ed.; American Scientific Publishers: Valencia, CA, 2004; Vol. 2, p 475.
(3) Endres, R. G.; Cox, D. L.; Singh, R. R. P. *Rev. Mod. Phys.* **2004**, *76*, 195.
(4) *Lecture Notes in Physics*; Cuniberti, G., Fagas, G., Richter, K., Eds.; Springer: Berlin, Germany, 2005; Vol. 68.
(5) (a) Xu, B.; Zhang, P.; Li, X.; Tao, N. J. *Nano Lett.* **2004**, *4*, 1105. (b) Cohen, H.; Nogues, C.; Naaman, R.; Porath, D. *Proc. Natl. Acad. Sci. U.S.A.* **2005**, *102*, 11589. (c) Van Zalinge, H.; Schiffrin, D. J.; Bates, A. D.; Haiss, W.; Ulstrup, J.; Nichols, R. J. *ChemPhysChem* **2006**, *7*, 94.
(6) Cohen, H.; Sapir, T.; Borovok, N.; Molotsky, T.; Di Felice, R.; Kotlyar, A. B.; Porath, D. *Nano Lett.* **2007**, *7*, 981.
(7) Shapir, E.; Calzolari, A.; Cavazzoni, C.; Ryndyk, D.; Cuniberti, G.; Kotlyar, A. B.; Di Felice, R.; Porath, D. *Nat. Mater.* **2008**, *7*, 68.
(8) We neglect, in the context of this study, the metallization of DNA intended as wrapping the double helix with a thick external cable or by a series of nanoparticles, such as, for example, in: (a) Braun, E.; Eichen, Y.; Sivan, U.; Ben-Yoseph, G. *Nature* **1998**, *391*, 775. (b) Richter, J.; Mertig, M.; Pompe, W.; Mnch, I.; Schackert, H. K. *Appl. Phys. Lett.* **2001**, *78*, 536. (c) Berti, L.; Alessandrini, A.; Facci, P. *J. Am. Chem. Soc.* **2005**, *127*, 11216. (d) Maubach, G.; Born, D.; Csáki, A.; Fritzsche, W. *Small* **2005**, *1*, 619. (e) We devote our attention only to the interaction of base pairs with single transition-metal ions.
(9) Burda, J.; Šponer, J.; Hobza, P. *J. Phys. Chem.* **1996**, *100*, 7250.
(10) Burda, J. V.; Špiner, J.; Leszczynski, J.; Hobza, P. *J. Phys. Chem. B* **1997**, *101*, 9670.
(11) Rulisek, L.; Sponer, J. *J. Phys. Chem. B* **2003**, *107*, 1913.
(12) Noguera, M.; Bertran, J.; Sodupe, M. *J. Phys. Chem. A* **2004**, *108*, 333.
(13) Di Felice, R.; Calzolari, A.; Zhang, H. Y. *Nanotechnology* **2004**, *15*, 1256.
(14) Fuentes-Cabrera, M.; Sumpter, B. G.; Šponer, J. E.; Šponer, J.; Petit, L.; Wells, J. C. *J. Phys. Chem. B* **2007**, *111*, 870.
(15) Pavelka, M.; Shukla, M. K.; Leszczynski, J.; Burda, J. V. *J. Phys. Chem. A* **2008**, *112*, 256.
(16) Alexandre, S. S.; Soler, J. M.; Seijo, L.; Zamora, F. *Phys. Rev. B* **2006**, *73*, 205112.
(17) Noguera, M.; Branchadell, V.; Costantino, E.; Ríos-Font, R.; Sodupe, M.; Rodríguez-Santiago, L. *J. Phys. Chem. A* **2007**, *111*, 9823.
(18) (a) Jensen, R. H.; Davidson, N. *Biopolymers* **1966**, *4*, 17. (b) Daune, M.; Dekker, C. A.; Schachman, H. K. *Biopolymers* **1966**, *4*, 51. (c) Eichhorn, G. L.; Butzow, J. J.; Clark, P.; Tarien, E. *Biopolymers* **1967**, *5*, 283. (d) Dattagupta, N.; Crothers, D. M. *Nucleic Acids Res.* **1981**, *9*, 2971. (e) Lee, J. S.; Latimer, L. J. P.; Reid, R. S. *Biochem. Cell. Biol.* **1993**, *71*, 162.
(19) Rakitin, A.; Aich, P.; Papadopoulos, C.; Koubzar, Y.; Vedeneev, A. S.; Lee, J. S.; Xu, J. M. *Phys. Rev. Lett.* **2001**, *86*, 3670.
(20) Aich, P.; Labiuk, S. L.; Tari, L. W.; Delbaere, L. J. T.; Roesler, W. J.; Falk, K. J.; Steer, R. P.; Lee, J. S. *J. Mol. Biol.* **1999**, *294*, 477.
(21) Kool, E. T. *Acc. Res* **2002**, *35*, 936.
(22) Tanaka, K.; Tengeiji, A.; Kato, T.; Toyama, N.; Shionoya, M. *Science* **2003**, *299*, 1212.
(23) Wagenknecht, H.-A. *Angew. Chem., Int. Ed.* **2003**, *42*, 3204.
(24) Wengel, J. *Org. Biomol. Chem.* **2004**, *2*, 277.
(25) Moreno-Herrero, F.; Herrero, P.; Moreno, F.; Colchero, J.; Gómez-Navarro, C.; Gómez-Herrero, J.; Baró, A. M. *Nanotechnology* **2003**, *14*, 128.

(26) Omerzu, A.; Mihailovic, D.; Anelak, B.; Turel, I. *Phys. Rev. B* **2007**, *75*, 121103.

(27) Zhang, H. Y.; Calzolari, A.; Di Felice, R. *J. Phys. Chem. B* **2005**, *109*, 15345.

(28) Lippard, S. J. In *Bioinorganic Chemistry*; Bertini, I., Gray, H. B., Lippard, S. J., Valentine, J. S., Eds.; University Science Books: Mill Valley, CA, 1994; p 564, and references therein.

(29) Lippert, B. *Coord. Chem. Rev.* **2000**, *200*−*202*, 487.

(30) Brabec, V.; Vrána, O.; Nováková, O.; Kleinwächter, V.; Intini, F. P.; Coluccia, M.; Natile, G. *Nucleic Acids Res.* **1996**, *24*, 336.

(31) Zamora, F.; Sabat, M. *Inorg. Chem.* **2002**, *41*, 4976.

(32) Šponer, J.; Leszczynski, J.; Hobza, P. *J. Mol. Struct.: THEOCHEM* **2001**, *573*, 43.

(33) Šponer, J.; Sabat, M; Burda, J. V.; Leszczynski, J.; Hobza, P; Lippert, B. *J. Biol. Inorg. Chem.* **1999**, *4*, 537.

(34) Šponer, J.; Sabat, M.; Burda, J. V.; Leszczynski, J.; Hobza, P. *J. Phys. Chem. B* **1999**, *103*, 2528.

(35) Krizanovic, O.; Sabat, M.; Beyerle-Pfnür, R.; Lippert, B. *J. Am. Chem. Soc.* **1993**, *115*, 5538.

(36) Moroni, F.; Famulari, A.; Raimondi, M.; Sabat, M. *J. Phys. Chem. B* **2003**, *107*, 4196.

(37) Carloni, P.; Andreoni, W. *J. Phys. Chem.* **1996**, *100*, 17797.

(38) Vallee, B. L.; Falchuk, K. H. *Physiol. Rev.* **1993**, *73*, 79.

(39) (a) Carloni, P.; Sprik, M.; Andreoni, W. *J. Phys. Chem. B* **2000**, *104*, 823. (b) Spiegel, K.; Rothlisberger, U.; Carloni, P. *J. Phys. Chem. B* **2004**, *108*, 2699.

(40) (a) Rosenberg, B.; VanCamp, L.; Krigas, T. *Nature* **1965**, *205*, 698. (b) Rosenberg, B.; VanCamp, L.; Trosko, J. E.; Mansour, V. H. *Nature* **1969**, *222*, 385. (c) Sherman, S. E.; Gibson, D.; Wang, A. H.; Lippard, S. J. *Science* **1985**, *230*, 412. (d) Lippert, B. *Cisplatin: Chemistry and Biochemistry of a Leading Anticancer Drug*, 1st ed.; Wiley-VCH: Weinheim, Germany, 1999.

(41) Sternberg, U.; Koch, F.-T.; Bräuer, M.; Kunert, M.; Anders, E. *J. Mol. Model.* **2001**, *7*, 54.

(42) Becke, A. D. *J. Chem. Phys.* **1993**, *98*, 5648.

(43) See, for example: (a) Ricca, A.; Bauschlicher, C. W. *Chem. Phys. Lett.* **1995**, *245*, 150. (b) Blomberg, M. R. A.; Siegbahn, P. E.; Svensson, M. *J. Chem. Phys.* **1996**, *104*, 9546. (c) Barone, V.; Adamo, C.; Mele, F. *Chem. Phys. Lett.* **1996**, *249*, 290. (d) Holthausen, M. C.; Mohr, M.; Koch, W. *Chem. Phys. Lett.* **1995**, *240*, 245. (e) Sodupe, M.; Branchadell, V.; Rosi, M.; Bauschlicher, C. W. *J. Phys. Chem. A* **1997**, *101*, 7854. (f) Luna, A.; Alcami, M.; Mo, O.; Yanez, M. *Chem. Phys. Lett.* **2000**, *320*, 129. (g) Bauschlicher, C. W.; Ricca, A.; Partridge, H.; Langhoff, S. R. In *Recent Advances in Density Functional Theory, Part II*; Chong, D. P., Ed.; World Scientific Publishing Co.: Singapore, 1997.

(44) Figgen, D.; Rauhut, G.; Dolg, M.; Stoll, H. *Chem. Phys.* **2005**, *311*, 227.

(45) Frisch, M. J. Trucks, G. W.; Schlegel, H. B.; Scuseria, G. E.; Robb, M. A.; Cheeseman, J. R.; Montgomery, J. A., Jr.; Vreven, T.; Kudin, K. N.; Burant, J. C.; Millam, J. M.; Iyengar, S. S.; Tomasi, J.; Barone, V.; Mennucci, B.; Cossi, M.; Scalmani, G.; Rega, N.; Petersson, G. A.; Nakatsuji, H.; Hada, M.; Ehara, M.; Toyota, K.; Fukuda, R.; Hasegawa, J.; Ishida, M.; Nakajima, T.; Honda, Y.; Kitao, O.; Nakai, H.; Klene, M.; Li, X.; Knox, J. E.; Hratchian, H. P.; Cross, J. B.; Bakken, V.; Adamo, C.; Jaramillo, J.; Gomperts, R.; Stratmann, R. E.; Yazyev, O.; Austin, A. J.; Cammi, R.; Pomelli, C.; Ochterski, J. W.; Ayala, P. Y.; Morokuma, K.; Voth, G. A.; Salvador, P.; Dannenberg, J. J.; Zakrzewski, V. G.; Dapprich, S.; Daniels, A. D.; Strain, M. C.; Farkas, O.; Malick, D. K.; Rabuck, A. D.; Raghavachari, K.; Foresman, J. B.; Ortiz, J. V.; Cui, Q.; Baboul, A. G.; Clifford, S.; Cioslowski, J.; Stefanov, B. B.; Liu, G.; Liashenko, A.; Piskorz, P.; Komaromi, I.; Martin, R. L.; Fox, D. J.; Keith, T.; Al-Laham, M. A.; Peng, C. Y.; Nanayakkara, A.; Challacombe, M.; Gill, P. M. W.; Johnson, B.; Chen, W.; Wong, M. W.; Gonzalez, C.; Pople, J. A. *Gaussian 03*, revision C.02; Gaussian, Inc.: Wallingford, CT, 2004.

(46) Šponer, J.; Burda, J. V.; Sabat, M.; Leszczynski, J.; Hobza, P. *J. Phys. Chem. A* **1998**, *102*, 5951.

(47) On the basis of a M−DNA model structure proposed by Lee and co-workers,[19] for the Zn(II)−GC imino complex, we examined a four-fold coordination structure of the Zn cation with the N_1^G, N_3^C, and O_6^G of the bases and the O atom of one added water molecule. The relaxed structure has a distorted tetrahedral arrangement of the atoms. The addition of two water molecules in the Zn(II)−GC imino complex has also been investigated, yielding the Lee penta model by Fuentes-Cabrera and coworkers;[14] the arrangement for the five-fold-coordinated Zn(II) configuration is trigonal bipyramid, that is, even farther from planarity and not considered in our work. Among the possible Zn(II)−GC imino complexes, another model has been proposed by Alexandre and coworkers:; this model is very different from the Lee model because it is neutral (due to the addition of a OH^- group), and the Zn ion is placed in the major instead of the minor groove. For the Cu(II) ion, a d^9 open-shell cation, among the four-fold coordination geometries, the square planar is known to be the preferred one, especially for small size ligands. Therefore, we have examined mainly the Cu(II)−imino complex with the metal in a square planar coordination with the N_1^G, N_3^C, O_6^G, and O_2^C atoms of the bases. We also considered a four-fold coordination with the N_1^G and N_3^C atoms of the bases and the O atoms of two added water molecules. The relaxed structure in the latter case has a distorted tetrahedral arrangement of the atoms.

(48) (a) Sugiyama, H.; Saito, I. *J. Am. Chem. Soc.* **1996**, *118*, 7063. (b) Mehrez, H.; Anantram, M. P. *Phys. Rev. B* **2005**, *71*, 115405. (c) Rösch, N.; Voityuk, A. A. *Top. Curr. Chem.* **2004**, *237*, 37.

(49) (a) Perdew, J. P.; Burke, K.; Ernzerhof, M. *Phys. Rev. Lett.* **1996**, *77*, 3865. (b) Perdew, J. P.; Burke, K.; Ernzerhof, M. *Phys. Rev. Lett.* **1997**, *78*, 1396. (c) Adamo, C.; Barone, V. *J. Chem. Phys.* **1999**, *110*, 6158.

(50) (a) Singh, U. C.; Kollman, P. A. *J. Comput. Chem.* **1984**, *5*, 129. (b) Besler, B. H., Jr.; Kollman, P. A. *J. Comput. Chem.* **1990**, *11*, 431.

(51) Dreizler, R. M.; Gross, E. K. U. *Density Functional Theory. An Approach to the Quantum Many-Body Problem*; Springer-Verlag: Berlin, Germany, 1990.

(52) Corni, S.; De Rienzo, F.; Di Felice, R.; Molinari, E. *Int. J. Quantum Chem.* **2005**, *102*, 328.

JP806419T